# Studies on the Reactions of CH($v$=0 and 1) with NO and $O_2$

Satoru OKADA, Katsuyoshi YAMASAKI, †† Hiroyuki MATSUI,* Ko SAITO,† and Kazumasa OKADA†
Department of Reaction Chemistry, Faculty of Engineering, The University of Tokyo, Hongo, Tokyo 113
†Department of Chemistry, Hiroshima University, Kagamiyama, Higashi-Hiroshima 724

(Received August 21, 1992)

Rate constants for the reactions of CH($X^2\Pi$: $v$=0,1) with NO and $O_2$ are measured under pseudo-first-order conditions at 297±5 K. CH($X^2\Pi$: $v$=0,1) radicals are generated by excimer laser photolysis of $CHBr_3$ and $(CH_3)_2CO$ at 193 nm, and detected by the laser-induced fluorescence (LIF) technique. The overall rate constants obtained at the total pressure of 20 Torr Ar are: $k_{NO}(v=0)=(1.6\pm0.2)\times10^{-10}$, $k_{NO}(v=1)=(1.3\pm0.6)\times10^{-10}$, $k_{O_2}(v=0)=(3.5\pm0.3)\times10^{-11}$, and $k_{O_2}(v=1)=(3.4\pm0.8)\times10^{-11}$ ($cm^3$ $molecule^{-1}$ $s^{-1}$).

No apparent pressure dependence is indicated for the rate constants over the pressure range of 5—50 Torr Ar for CH+NO, and 5—30 Torr Ar for CH+$O_2$ reactions, respectively.

The reaction mechanisms are discussed based on the quantum mechanical calculations of the potential energy surfaces of CH+NO and CH+$O_2$ systems.

The methylidyne radical (CH) is believed to play important roles in the formation of prompt $NO_x$ or electronically excited and ionic species in combustion processes, because of its high heat of formation and reactivity: Detailed examinations of CH radicals in hydrocarbon/air flame have already been performed by using laser absorption[1] and laser-induced fluorescence (LIF)[2] methods for the ground state of CH, and by using the emission spectroscopy[1,3] for the electronically excited state. The CH+$N_2$ reaction producing N+HCN at high temperatures is believed to be the source of "prompt" NO,[4,5] and it has been predicted[6] that the formation and conversion of NO by the reaction with CH is one of the most important kinetic steps in N-containing flames.

The CH+$O_2$ reaction leading to the formation of OH is sufficiently exoergic to produce the OH in its electronically excited state: Chemiluminescence for ($A^2\Sigma^+$–$X^2\Pi$) transition has been examined.[3,7] The reaction of CH with O atoms was indicated to have an important contribution to the initial stage of soot formation[8] via the production of ionic species such as $HCO^+$.[9]

The CH+NO reaction system was first investigated by Lin:[10] CO vibrational inverted emission at 5 μm was observed in vacuum UV flash photolysis of $CHBr_3$/NO mixtures and he suggested the possibility of direct formation of vibrationally excited CO and NH from the CH+NO reaction. Lin and co-workers[7,11] employed UV laser photolysis of $CHBr_3$ to generate CH and LIF method to probe CH and to measure the overall consumption rate of CH. The rate constant for the CH+NO reaction was found to be $k_{NO}=(1.9\pm0.3)\times10^{-10}$ $cm^3$ $molecule^{-1}$ $s^{-1}$ and independent of temperature.[12] They also estimated the rate constant from the time dependence of chemiluminescence intensity for NH ($A^3\Pi$–$X^3\Sigma^-$). They obtained the value of $k_{NO}=(2.5\pm0.5)\times10^{-10}$ $cm^3$ $molecule^{-1}$ $s^{-1}$ which is in close agreement with that obtained from the decay rate of CH. Thus, they postulated NH ($A^3\Pi$) to be directly generated from the CH+NO reaction.[7] Wagal et al.[13] who produced CH by IRMPD of $CH_3NH_2$ and cyclo-$C_3H_6$ obtained the rate constant $k_{NO}=(2.0\pm0.3)\times10^{-10}$ $cm^3$ $molecule^{-1}$ $s^{-1}$. Despite the different source for CH, the rate constants for the CH+NO reaction reported thus far agree each other quite well and are found as fast as near the gas kinetic collision rate. Nishiyama et al.[14] who produced CH from the $C(^1D)+H_2$ reaction in fast flow system, observed NH ($A^3\Pi$–$X^3\Sigma^-$) chemiluminescence and measured the internal energy state distribution in NH ($A^3\Pi$) state from the dispersed emission spectrum. They suggested the direct four-center mechanism for the CH+NO reaction leading to formation of NH ($A^3\Pi$).

Recently, Dean et al.[15] studied this reaction using laser absorption technique behind shock waves in the pyrolysis of $C_2H_6$/NO and $CH_4$/NO mixtures. They compared the time dependences and the absolute concentrations of CH, NH, and OH with and without addition of NO to $CH_4$ and $C_2H_6$ and extracted the information regarding the reactions of CH+NO from such comparison through kinetic simulation. They concluded that both the reaction channels for producing NH and OH are minor; this conclusion is consistent with that of Miller and Bowman,[16] who examined the reaction mechanisms from theoretical bases and indicated that HCN+O are the major products.

Bozzelli et al. estimated the branching fractions for this reaction using quantum Kassel theory (which is designated as QRRK theory by Dean[17]) with potential energy surfaces estimated based on microscopic reversibility for reverse reactions, or on analogies to carbene H shifts for isomerization of the reaction intermediates.[18] According to their calculation, reaction channels are not selective, but many products which are thermochemically acceptable combinations are possible, i.e., the branching fractions at room temperature are; 0.56 for N+HCO, 0.22 for H+NCO, 0.15 for O+HCN, 0.04

††Present address: Department of Chemistry, Niigata Univ., Niigata.

for NH+CO, and 0.04 for OH+CN channels, respectively.

Studies of the CH+$O_2$ reaction system were also initiated by Lin.[19] Not only CO laser emission at 5 μm but strong $CO_2$ laser emission at 10 μm was observed in vacuum UV flash photolysis of $CHBr_3/O_2$ mixtures: it was postulated that the CH+$O_2$ reaction directly produces both vibrationally excited CO and $CO_2$.

Subsequently, the rate constant for the CH+$O_2$ reaction was measured in several experimental studies.[7,11,12,20—23] The results, ranging $k_{O_2}$ = (2—6)×$10^{-11}$ $cm^3$ $molecule^{-1}$ $s^{-1}$, roughly agreed each other despite the different method for generation of CH (UV photolysis of $CHBr_3$,[7,11,12] $CH_2Br_2$,[23] or $CHClBr_2$,[23] IRMPD of $CH_3$ $NH_2$,[20] and sequential Br atom abstraction from $CHBr_3$ with excess alkali-metal atoms[22]); the rate constant has been found to be independent of temperature.[12] Only Duncanson et al.[21] has reported an order of magnitude smaller value than others, but the source of this discrepancy is still unknown. Messing et al.[20] and Lichtin et al.[7] measured the rate constant from the decay rate of OH ($A^2\Sigma^+$–$X^2\Pi$) chemiluminescence: it was in reasonable agreement with that obtained from the decay rate of CH, and postulated OH ($A^2\Sigma^+$) to be directly generated by the CH+$O_2$ reaction.

Although the rate constants for the overall consumption of CH by various stable molecules were measured extensively,[24] the details of the reaction mechanisms have not been clarified. Since there has been no direct experimental evidence on the main product channel(s) of CH+NO and CH+$O_2$ reactions, it will be important to detect radicals of concern so as to examine these contradicting prediction.

In this study, the reaction rate constants of CH with and without vibrational excitation in the reactions CH+NO and CH+$O_2$ are measured. Search for the reaction products in these systems is also tried. In addition, quantum mechanical calculations were performed in order to examine the mechanisms for these reactions.

No previous measurement on the rate constant for vibrationally excited CH with NO reaction has been reported.

Duncanson et al.[21] reported that the rate constant for CH($v$=1)+$O_2$ is about two times larger than that for CH($v$=0). But these rate constants are much less than those of other measurements for the reaction CH($v$=0)+$O_2$. If there exists appreciable vibrational energy dependence on the rate constants, such informations should reflect detailed dynamic features of the reactive collision: thus reinvestigation on these reaction systems seems to be important to get insight into the details of the reaction mechanisms.

## Experimental

A standard pump-probe laser technique in a quasi-static cell was used to examine the reactions of CH radicals. An ArF excimer laser (Questek 2220: duration, 10 ns; repetition 7—15 Hz) was used as the photolysis source with a typical pulse energy of 3—5 mJ/pulse in a 0.6 cm diameter beam.

$CHBr_3$ was mainly used as the precursor of CH radicals because of the high efficiency in generating CH radicals. In order to examine the effect of the precursor molecules on the measured reaction rate constants, $(CH_3)_2CO$ was also used as a source of CH. The production of CH radicals from $CHBr_3$ is found to be over 50 times more efficient than $(CH_3)_2CO$.

A XeCl (308 nm) excimer laser (Lambda Physik LPX110i) pumped dye laser (PRA DL14P: duration, 10 ns; typical pulse energy, 50—100 μJ/pulse; linewidth, 0.8 $cm^{-1}$), with a KDP doubling crystal was utilized to get LIF excitation spectra of radicals.

A photomultiplier tube (Hamamatsu R374) was used to detect LIF with cut-off filters (Corning CS2-58 or Ritsu UV-39) or UV (Toshiba UV-D33S) filters to reduce the scattered photolysis laser light. Signals from the photomultiplier tube were fed into a gated integrator/boxcar averager (Stanford Research Systems SR250) and processed with a laboratory microcomputer (Epson PC286).

Radicals detected by LIF method in this work are listed in Table 1. HCO could not be detected in the photolysis of $CHBr_3/NO$ nor $CHBr_3/O_2$ mixtures. The detection limit of HCO for the present LIF system was estimated to be at least $10^{13}$ molecules $cm^{-3}$:[25,26] Typical concentrations of HCO in this experimental conditions were much less than the detection limit.

The partial pressure of each component in sample gas mixtures was evaluated by use of a capacitance manometer (MKS 122AA-00100AB) with a pressure-flux calibration curve. Most experiments were conducted under the condition of flowing gas mixture (>40 cm $s^{-1}$) in order to minimize the interference by the photolysis and reaction products. Typical partial pressures of $CHBr_3$ and $(CH_3)_2CO$ were 0.8 mTorr and 3.4 mTorr, respectively, and partial pressure ranges of NO and $O_2$ were 0—30 mTorr and 0—250 mTorr, respectively (1 Torr=133 Pa). The initial concentrations of CH precursors were sufficiently small to ensure the pseudo-first-order reaction conditions that $[CH]_{t=0}$<<[NO] or $[O_2]$. The total pressure ranges were 5—100 Torr for CH+NO and 5—30 Torr for CH+$O_2$ reactions using Ar as a buffer gas. All the experiments were carried out at room temperature (297±5 K).

$CHBr_3$ (Tokyo Kasei: 99.0%), which contains 50 ppm of diphenylamine as stabilizer, was purified by trap-to-trap distillation to remove colored non-volatile components and degassed at 298 K to remove water. $(CH_3)_2CO$ (Kanto Chemical: 99%) was only degassed before using. NO (Takachiho Kagaku: 99.9%), $O_2$ (Nihon Sanso: 99.99%) and Ar (Nihon Sanso: 99.9999%) were used without further purification. All sample gases were diluted in argon and stored in glass bulbs.

## Results

The LIF excitation spectrum for CH ($A^2\Delta$–$X^2\Pi$) observed at 10 μs after the photolysis is shown in Fig. 1. In addition to the (0–0) vibrational band Q and R branches, the (1–1) and (2–2) vibrational bands Q and R branches are shown in this chart.[27]

Table 1. Summary of Radicals Detected by LIF

| Radical | Transition | $\lambda$/nm | Laser Dye | Lines utilized to monitor the time profiles |
|---|---|---|---|---|
| CH | $A^2\Delta$–$X^2\Pi$ | 430 | S-420 | (0–0) $R_2(1/2)$, (1-1) $R_1(3/2)$ |
| NH | $A^3\Pi$–$X^3\Sigma^-$ | 334 | DCM/KDP | (0–0) $R_1(4)$ |
| NH | $c^1\Pi$–$a^1\Delta$ | 326 | DCM/KDP | (0–0) P(3) |
| CN | $B^2\Sigma^+$–$X^2\Sigma^+$ | 387 | BBQ | (0–0) $R_1(11/2)+R_2(9/2)$ |
| OH | $A^2\Sigma^+$–$X^2\Pi$ | 308 | R-640/KDP | (0–0) $Q_1(3/2)$ |
| NCO | $A^2\Sigma^+$–$X^2\Pi$ | 417 | S-420 | (100)–(000) |

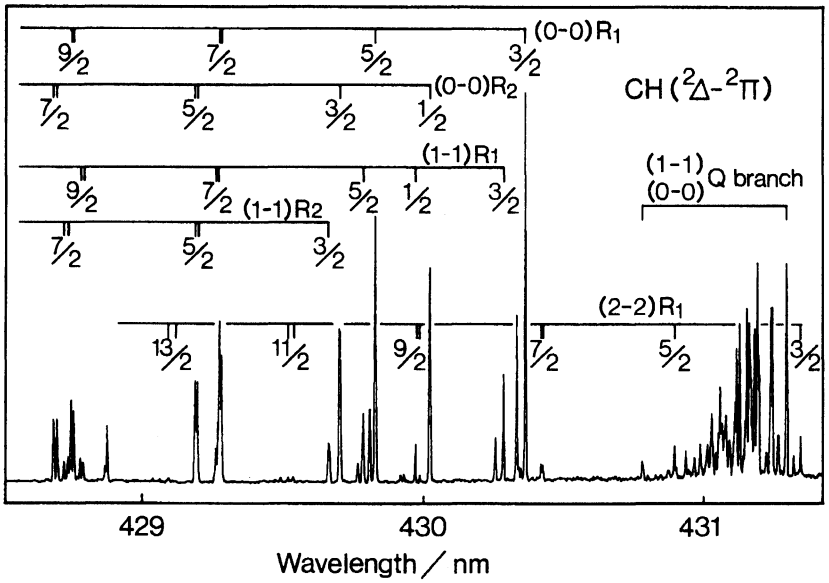


Fig. 1. LIF excitation spectrum of CH. $P(CHBr_3)$=2.6 mTorr, $P_{Tot}(Ar)$=20 Torr; $t$=10 μs after the photolysis.

The Boltzmann plots for the vibrational distribution at 5, 10, and 40 μs after the photolysis for $R_1$ (3/2) line in (0–0), (1–1), and (2–2) bands are shown in Fig. 2, where the relative populations were estimated with corrections for Franck–Condon factors[28] and the sensitivity factors against wavelength. The vibrational temperature was found to be almost constant within 2930±260 K ($2\sigma$) at $P$=20 Torr (Ar) for $t$=0—40 μs, showing that the vibrational relaxation of CH is very slow in this time interval, meanwhile, the observed LIF intensities showed substantial decrement at 40 μs for the typical experimental conditions.

Therefore, it is confirmed that vibrational deactivation is not responsible for the observed decay of excited CH radicals.

The wavelength of the dye laser was tuned to $R_1$ (3/2) or $R_2$ (1/2) lines when the time profiles of CH LIF intensity were monitored. Typical time dependences of CH LIF intensity in some mixtures of $CHBr_3$/NO/Ar are shown in Fig. 3. The decay profile of the CH LIF intensity was fitted to the single exponential formula which gave the pseudo-first-order decay rate of CH, $\tau_d^{-1}$. Plots of $\tau_d^{-1}$ versus NO and $O_2$ concentrations showed good linear correlations as shown in Fig. 4, and the intercept which usually represents the rate for the reaction with the precursor molecules and/or the heterogeneous reaction at the wall was confirmed to be sufficiently small.

The overall rate constants for the reactions CH($X^2\Pi$ : $v$=0,1)+NO and CH($X^2\Pi$ : $v$=0,1)+$O_2$→products, measured at the total pressure of 20 Torr Ar, are summarized in Tables 2 and 3, respectively. Present results for the overall rate constants for these two reactions were consistent with previous works.

Pressure dependence of the rate constants was also measured. For CH($v$=0)+NO→products, the covered pressure range was 5 to 50 Torr Ar, and the decay rate of CH showed no systematic pressure dependence. The rate constant averaged over for all the pressure range is $(1.6\pm0.2)\times10^{-10}$ $cm^3$ $molecule^{-1}$ $s^{-1}$.

For CH($v$=0,1)+$O_2$, the rate constants were measured at 5 and 30 Torr Ar in addition to that at 20 Torr. The rate constants for CH($v$=0)+$O_2$→products were $(3.90\pm0.60)\times10^{-11}$, and $(4.28\pm0.30)\times10^{-11}$ $cm^3$ $molecule^{-1}$ $s^{-1}$ at 5 and 30 Torr, respectively. Those for CH($v=1$) + $O_2$ were $(4.30\pm0.04)\times10^{-11}$, and $(3.88\pm1.00)\times10^{-11}$ $cm^3$ $molecule^{-1}$ $s^{-1}$ at 5 and 30 Torr, respectively.

The rate constants for CH+NO and CH+$O_2$ do not have obvious dependence on the total pressure nor on the vibrational energy for $v$=0 or 1. Also, changing

Table 2. Rate Constant for $CH(X^2\Pi)+NO$

| $k$/cm$^3$ molecule$^{-1}$ s$^{-1}$ | $P_{Tot}$/Torr | $T$/K | Reference |
|---|---|---|---|
| $(2.9\pm0.7)\times10^{-10}$ | 100(Ar) | Room temp | 11 |
| $(1.9\pm0.3)\times10^{-10}$ | 100(Ar) | 297—676 | 12 |
| $(2.5\pm0.5)\times10^{-10}$ | 21(Ar) | Room temp | 7 |
| $(2.0\pm0.3)\times10^{-10}$ | 5(Ar) | 300 | 13 |
| $(1.61\pm0.18)\times10^{-10}$ | 20(Ar) | 297 | This work[1] ($v$=0) |
| $(1.30\pm0.41)\times10^{-10}$ | 20(Ar) | 297 | This work[2] ($v$=0) |
| $(1.30\pm0.60)\times10^{-10}$ | 20(Ar) | 297 | This work[1] ($v$=1) |

Errors denoted indicate $2\sigma$ deviation of the data. 1) $CHBr_3$ was used as the precursor for $CH(X^2\Pi)$. 2) $(CH_3)_2CO$ was used as the precursor for $CH(X^2\Pi)$.

Table 3. Rate Constant for $CH(X^2\Pi)+O_2$

| $k$/cm$^3$ molecule$^{-1}$ s$^{-1}$ | $P_{Tot}$/Torr | $T$/K | Reference |
|---|---|---|---|
| $(5.9\pm0.8)\times10^{-11}$ | 100(Ar) | Room temp | 11 |
| $(5.4\pm1.0)\times10^{-11}$ | 100(Ar) | 276—676 | 12 |
| $(3.3\pm0.4)\times10^{-11}$ | 10—30(Ar) | 298 | 20 |
| $(8.\ \pm3.\ )\times10^{-11}$ | 21(Ar) | Room temp | 7 |
| $(2.1\pm0.2)\times10^{-12}$ | 10(Ar) | Room temp | 21 |
| $(2.3\pm0.5)\times10^{-11}$ | 2(He) | 290 | 22 |
| $(5.1\pm0.3)\times10^{-11}$ | 2(Ar) | 297 | 23 |
| $(4.28\pm0.30)\times10^{-11}$ | 30(Ar) | 293 | This work ($v$=0) |
| $(3.88\pm1.00)\times10^{-11}$ | 30(Ar) | 293 | This work ($v$=1) |
| $(3.54\pm0.28)\times10^{-11}$ | 20(Ar) | 297 | This work ($v$=0) |
| $(3.37\pm0.78)\times10^{-11}$ | 20(Ar) | 293 | This work ($v$=1) |
| $(3.90\pm0.60)\times10^{-11}$ | 5(Ar) | 293 | This work ($v$=0) |
| $(4.30\pm0.04)\times10^{-11}$ | 5(Ar) | 293 | This work ($v$=1) |

Errors denoted indicate $2\sigma$ deviation of the data. $CHBr_3$ was used as the precursor for $CH(X^2\Pi)$.

the precursor molecules for generating CH radical from $CHBr_3$ to $(CH_3)_2CO$ brought no difference in the measured rate constant.

In addition to CH, LIF for NH ($A^3\Pi$–$X^3\Sigma^-$), NH ($c^1\Pi$–$a^1\Delta$), OH ($A^2\Sigma^+$–$X^2\Pi$), CN ($B^2\Sigma^+$–$X^2\Sigma^+$) and NCO ($A^2\Sigma^+$–$X^2\Pi$) were observed in $CHBr_3$/NO system, and LIF for $OH(A^2\Sigma^+$–$X^2\Pi)$ in $CHBr_3/O_2$ system. The intensity distribution of NH ($X^3\Sigma^-$) $R_1$ branch at 10 μs after the photolysis indicated that the rotational distribution was equilibrated at room temperature.

Examples of the time profiles of LIF intensities of radicals observed in $CHBr_3$/NO and $CHBr_3/O_2$ reaction systems are shown in Figs. 5(a) and 5(b), respectively.

In $CHBr_3$/NO reaction system, NH ($a^1\Delta$) was generated in the first ca. 5 μs after the photolysis and then decayed exponentially. Since no rising behavior corresponding to the decay of CH was seen, the generation of NH ($a^1\Delta$) may be due to the photolysis of the remaining reaction products in the cell and actually higher flowing rates of sample gas reduced the LIF intensity of NH ($a^1\Delta$).

Time profiles of NH ($X^3\Sigma^-$), CN and NCO showed a rise and decay behavior. The profile of NCO seems to have an induction time before the rapid increase and the rise rate did not agree with the decay rate of CH. The LIF intensities of NH ($X^3\Sigma^-$) and CN showed rise and decay profiles and could be fitted to a double exponential formula:

$$I_{LIF}/I_0 = A\exp(-{\tau_d}^{-1}t) - B\exp(-{\tau_r}^{-1}t) \quad (1)$$

where, ${\tau_r}^{-1}$ and ${\tau_d}^{-1}$ are the pseudo-first-order rise and decay rates, respectively, $I_0$ is the intensity of the dye laser, and $A$ and $B$ are the constants. The pseudo-first-order rise rates, ${\tau_r}^{-1}$, were plotted versus NO concentrations and found to be slower than the decay rates of CH in whole NO concentration range as shown in Fig. 4(a).

The present experiment may imply that neither NCO, NH($X^3\Sigma^-$), nor CN is one of the primary products of the CH+NO reaction, however, the reaction system is very complicated and one can not exclude the effects of side reactions (for example, the reactions NH+NO[29] and NCO+NO[30] are known to be very fast).

The mechanism of CH formation from $CHBr_3$ photodissociation by 193 nm laser photolysis is not clearly understood; it is probably produced by consecutive absorption of photons and C–Br bonds are broken successively. Thus, the concentrations of CHBr and $CHBr_2$

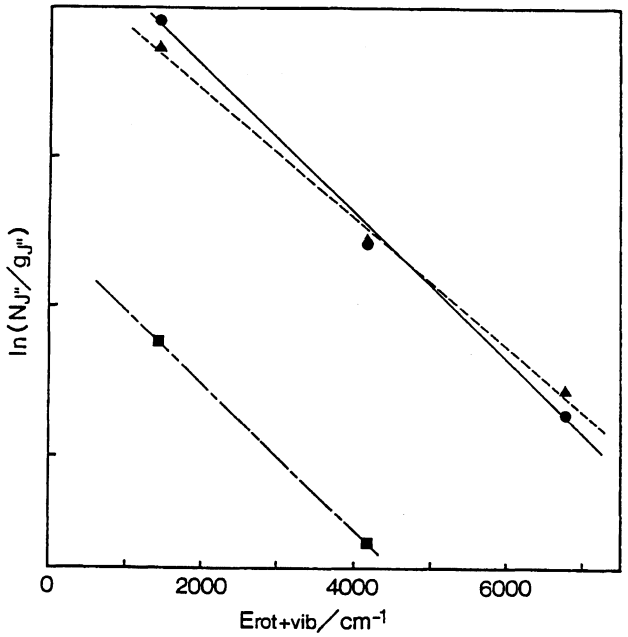


Fig. 2. Boltzmann plots of the vibrational distribution of CH observed at different delay times after the photolysis of $CHBr_3$ diluted in Ar. [●: $t=5$ μs, ▲: $t=10$ μs, ■: $t=40$ μs, $P(CHBr_3)=2.6$ mTorr, $P_{Tot}(Ar)=20$ Torr. Intensity of $R_1(3/2)$ line in (0–0), (1–1), and (2–2) vibrational bands was used for the plots. The straight lines represent the least-squares fit of the Boltzmann's plot. The vibrational temperatures were estimated as, 2710±260, 3140±300, and 2930 K for $t=5$, 10 and 40 μs, respectively.]

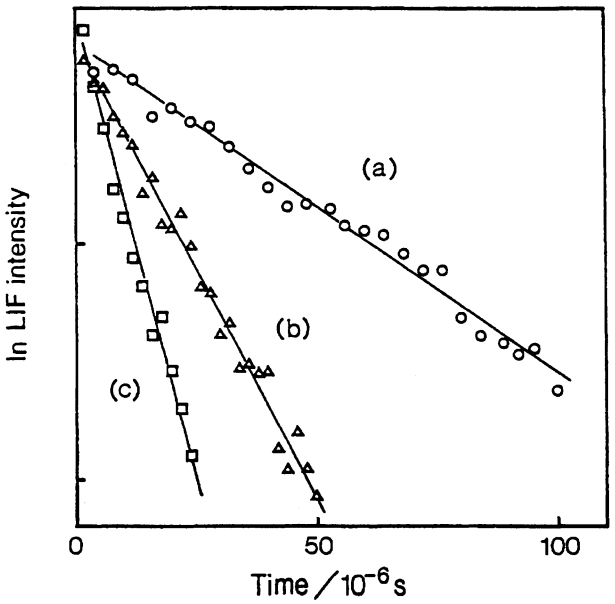


Fig. 3. Semi-log plots of the typical time profiles of CH LIF intensity. $P(CHBr_3)=0.8$ mTorr, $P_{Tot}(Ar)=$ 20 Torr; (a): $P(NO)=0$ mTorr, (b): $P(NO)=5.7$ mTorr, and (c): $P(NO)=13.4$ mTorr. The straight lines indicate the least-squares fit of the experimental data.

are expected to be much higher than that of CH. In addition, high concentration of CBr radical has been detected in the UV flash photolysis.[31] As these radicals are believed to be very reactive and should affect the observed profiles of product species.

Moreover, as the reaction is highly exothermic for these reaction channels, production rates of these radicals in their vibrational ground state can be different with the consumption rate of CH, if substantial fraction is produced in the vibrationally excited states and the relaxation is slow.

To check this possibility, $\tau_r$ for $NH(X^3\Sigma^-;\ v=0)$ was measured in total pressures ranging from 5 to 100 Torr under the constant NO concentration of $[NO]=(6.0\pm0.2)\times10^{14}$ molecules $cm^{-3}$. However, no clear pressure dependence of $\tau_r$ was indicated and the contribution of vibrationally excited $NH(X^3\Sigma^-)$ is not obvious.

OH was generated immediately after the sample mixtures were photolized and then gradually increased. The time profile of OH was simulated by using the observed time profile of NH ($X^3\Sigma^-$) in this work on the basis of the experimental result[29] that OH is directly produced in the reaction of NH ($X^3\Sigma^-$) with NO. Since this simulation well explain the time profile of OH as shown in Fig. 5(a) by solid line, the increase of OH after the photolysis in $CHBr_3$/NO reaction system can be due to the reaction of NH ($X^3\Sigma^-$) with NO.

It should be noted that precise discussion on the relative concentrations of these radicals may not be feasible; however, the relative concentrations of CH, NH ($X^3\Sigma^-$), CN, and OH were estimated from the relative LIF intensities considering the absorption coefficients and the quenching effects. From such evaluation, the branching fractions for NH ($v=0$), CN, and OH were estimated as 0.15, 0.002, and 0.2, respectively.

Since the amounts of CN and OH should be the same if they are produced only from the reaction of CH+NO directly, the difference in the observed concentrations should indicate the effects of successive reactions. In any case, the reaction channels producing NH, CN, and OH radicals are confirmed to be minor.

The relative concentration for NCO could not be estimated from the intensity of LIF excitation spectrum because of lack of the required informations; there remains a possibility that NCO is a major product for the reaction of CH+NO.

In $CHBr_3/O_2$ reaction system, OH was also generated just after the sample mixtures were photolized and then increased. The solid line in Fig. 5(b) is the profile for OH as a direct product calculated from the decay of CH: The formation rates of OH seems consistent with the observed dacay rate of CH. Thus, the possibility of OH as the primary product of the $CH+O_2$ reaction cannot be denied in this work. From the relative LIF intensities, the conversion of CH to $OH(v=0)$ was esti-

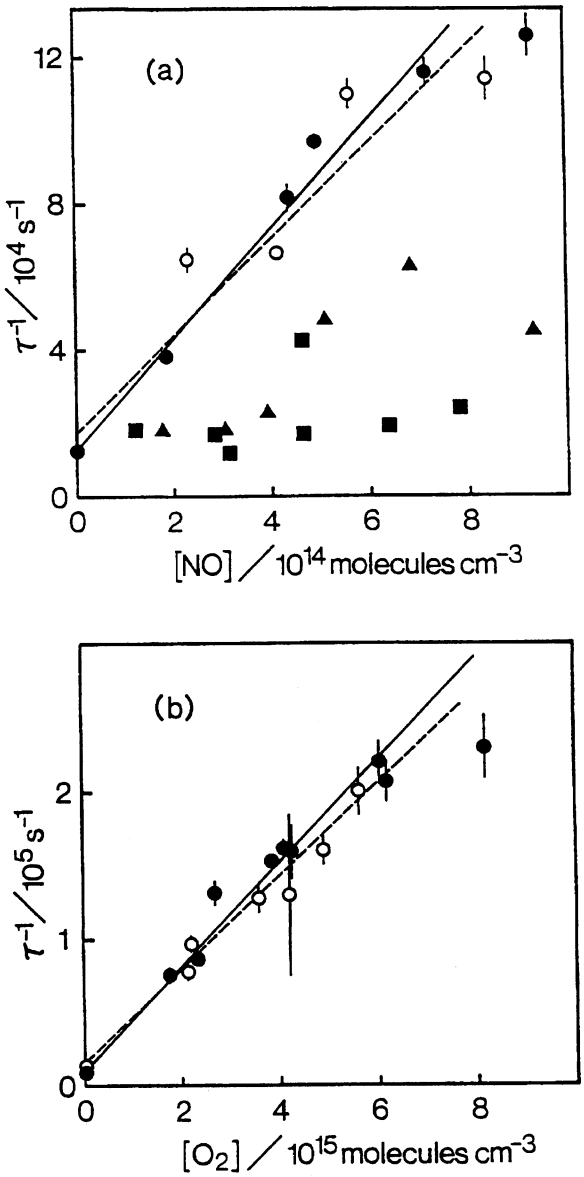


Fig. 4. Pseudo-first-order analysis for the decay rates of CH versus concentrations of NO (a), and $O_2$ (b). ●; experimental result for the decay rate of CH in the reactions of CH($v$=0)+NO and $O_2$, solid line; the least-squares fit of the experimental data. ○ ; experimental result for the decay rate of CH in the reactions of CH($v$=1)+NO and $O_2$, the dotted line; the least-squares fit of the experimental data. $P(CHBr_3)$=0.8 mTorr, $P_{Tot}(Ar)$=20 Torr. NH ($X^3\Sigma^-$) rise rate (▲) and CN rise rate (■) are shown for comparison in panel (a).

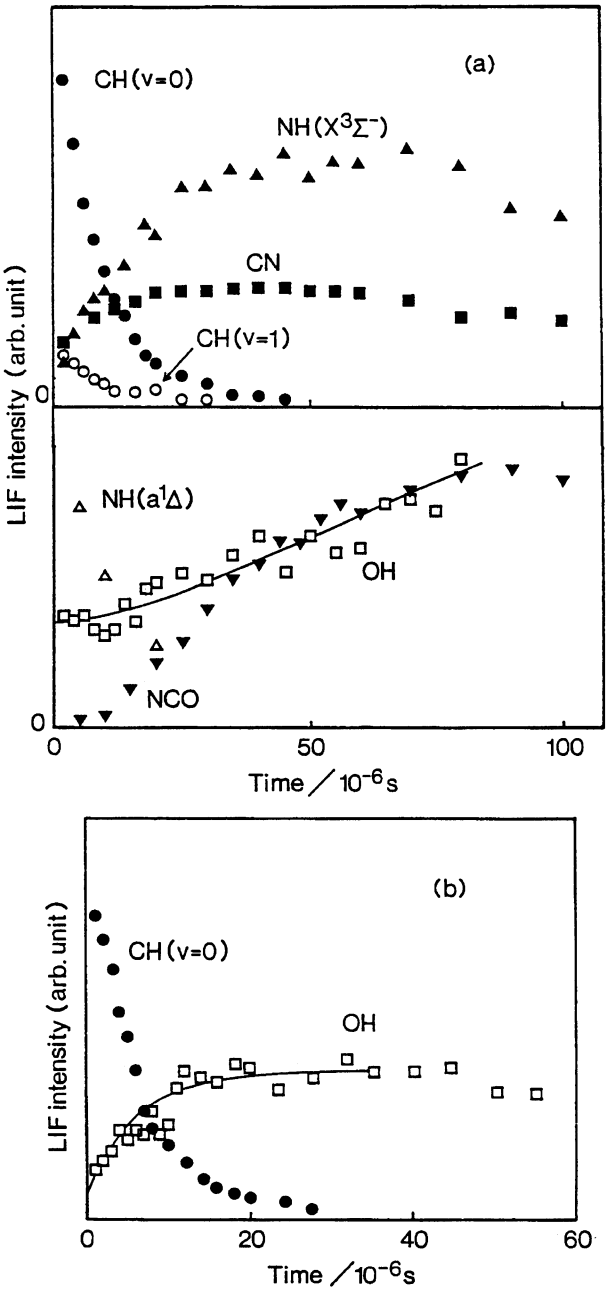


Fig. 5. Time profiles of radicals observed in the photolysis of (a) $CHBr_3/NO/Ar$ and (b) $CHBr_3/O_2/Ar$ mixtures. CH($v=0$):(●), CH($v=1$):(○), NH ($X^3\Sigma^-$):(▲), NH($a^1\Delta$):(△), CN:(■), OH:(□), and NCO (▼). Solid curves in panel (a) and (b) are the calculated profiles for OH postulating that they were produced in the NH($X^3\Sigma^-$)+NO and CH+$O_2$ reaction, respectively. $P(CHBr_3)$=0.8 mTorr, $P_{Tot}(Ar)$=20 Torr; (a) $P(NO)$=13.9 mTorr, the experimental conditions are the same in the upper and the lower panels, (b) $P(O_2)$=124 mTorr.

mated to be about 20%.

Further detailed examination will be required for the rest of products.

## Discussion

As for the product channels for the reactions CH+NO, no conclusive evidence has been presented so far.

Chemiluminescence from NH($A^3\Pi$) was observed by Lichten et al.[7] and Nishiyama et al.[14] Both of them have suggested that NH($A^3\Pi$) is formed via a direct four-center mechanism at room temperature.

In contrast, Dean et al.[15] observed absorption of

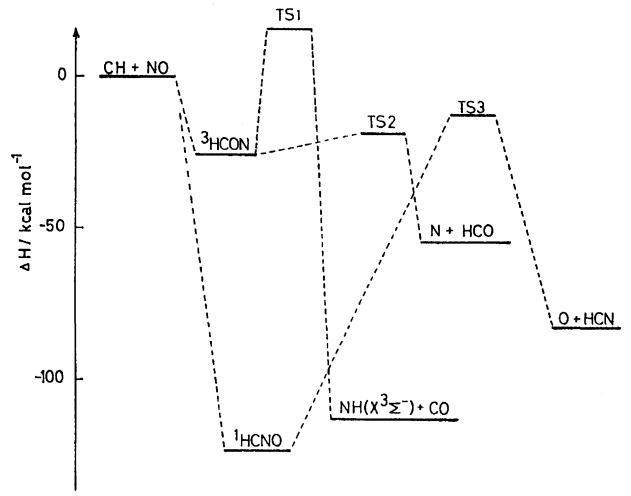


Fig. 6. Calculated potential energy diagrams for selected CH+NO reaction pathways. (MP4SDTQ/6-31G**//UHF/4-31G).

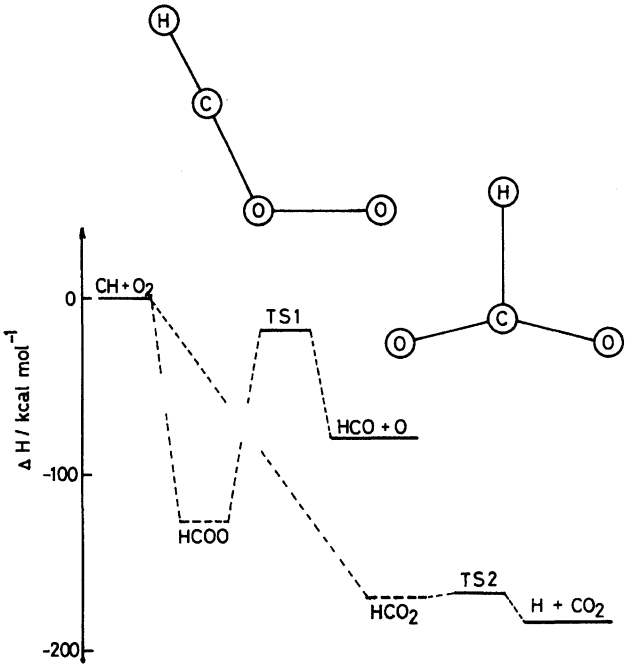


Fig. 7. Calculated potential energy diagrams for selected CH+O$_2$reaction pathways. (MP4SDTQ/6-31G**//UHF/4-31G).

$NH(X^3\Sigma^-)$ in the pyrolysis of $C_2H_6$/NO and $CH_4$/NO mixtures behind shock waves, and concluded that the branching fraction leading to the formation of NH $(X^3\Sigma^-)$ was suggested to be less than 10%.

Since NH $(A^3\Pi)$ should be quenched to NH $(X^3\Sigma^-)$ within a very short period (radiative lifetime = 404 ns[32]), formation of NH radicals (both in electronically excited and ground states) seems to be a minor channel, even if they are the direct products.

Also, the present LIF measurement on NH $(X^3\Sigma^-)$ indicates that the yield of NH in the CH+NO reaction is less than 15%, as was predicted by Dean et al.,[15] and Bozzelli et al.[18]

In order to examine the reaction mechanisms for CH–NO and CH–$O_2$ systems, potential energies for some reaction channels are estimated by ab initio calculation using MP4SDTQ/6-31G**//UHF/4-31G.

For the CH+NO reaction, three transition states ($TS_1$–$TS_3$) are found as shown in Fig. 6. The direct pathways leading to the formation of N+HCO and O+HCN seem possible.

The accuracy of the calculated potential surfaces may be judged from the energies of the stable products. The heats of reaction are evaluated as 113 (102), 55 (42), and 83 (72) kcal mol$^{-1}$ for the product channels $NH(X^3\Sigma^-)$+CO, N+HCO, and O+HCN, respectively, where, the values in the brackets are the heats of reaction given by Benson.[33] The difference of 11 to 13 kcal mol$^{-1}$ reaction energies between the ab initio calculation and the thermochemical data indicates that the branching fractions can not be determined accurately from these potential energy surfaces.

However, as shown in Fig. 6, the barrier height of $TS_2$ is indicated to be the lowest and implies that the reaction for producing N+HCO is dominated. If the relative energies for these transition states are correct each other, the present result is consistent with the conclusion of Bozzelli et al.[18] The amount of energy released in the formation of N+HCO is enough to dissociate HCO into H+CO, in the consecutive process, which might cause CO IR laser emission observed by Lin.[10]

For the reaction of CH+$O_2$, it is indicated that some fraction of CH is converted to OH directly, however, the transition state for this channel is not identified in this calculation.

With a very low energy barriers, CH+$O_2$ reaction leads to the formation of HCO+O($TS_1$) or H+$CO_2$($TS_2$), as shown in Fig. 7.

The reaction intermediates HCOO and $HCO_2$ are found, but the structures and the energies are not calculated here. The heats of reaction for CH+$O_2$→HCO+O and CH+$O_2$→H+$CO_2$ are calculated to be 80 and 185 kcal mol$^{-1}$, respectively, whereas, the corresponding energies calculated by thermochemical data are 73 and 184 kcal mol$^{-1}$, respectively;[33] this implies that the uncertainties of energies are less than 10 kcal mol$^{-1}$.

The energy barrier from $HCO_2$ to H+$CO_2$ has been estimated to be about 16 kcal mol$^{-1}$ and that to OH+CO to be about 33 kcal mol$^{-1}$.[34] The reaction pathway producing OH+CO may be possible via stable $HCO_2$ followed by migration of H, because the barrier is still about 150 kcal mol$^{-1}$ below the energy level of CH+$O_2$. In both reaction pathways the energy release is sufficient enough to excite the internal degrees of freedom of the product molecules, and furthermore, the OCO bond is so bent at the transition state leading to H+$CO_2$ that it is probable to cause strong vibrational excitation in $CO_2$. Intense IR emissions in $CO_2$ and CO observed by

Lin[19] may be explained by such a reaction scheme.

A comparison between the energies of these transition states suggests that the $CH+O_2$ reaction proceeds most likely to the formation of $H+CO_2$ and to $OH+CO$ via the $HCO_2$ intermediate.

Finally, as shown in Tables 2 and 3, the effect of vibrational excitation in CH on the rate constants for $CH+NO$ and $CH+O_2$ is found to be very small. Such conclusion is consistent with the present calculations because the barrier heights for all the transition states are much lower than the energies of the reactants.

The authors are grateful to the critical comments and discussion given by Professor M. C. Lin of Emory University, and Dr. A. M. Dean of Exxon Research and Engineering Co.

## References

1) R. G. Joklik, J. W. Daily, and W. J. Pitz, "21st Symp. Int. Combust., " The Combust. Inst., Pittsburg, PA, 1986, Abstr., p. 895.
2) R. J. Cattolica, D. Stepowski, D. Puechberty, and M. Cottereau, *J. Quant. Spectrosc. Radiat. Transfer*, **32**, 363 (1984).
3) A. G. Gaydon, "The Spectroscopy of Flames, " 2nd ed, Chapman and Hall, London (1974).
4) P. Glarborg, J. A. Miller, and R. J. Kee, *Combust. Flame*, **65**, 177 (1986).
5) M. R. Berman, and M. C. Lin, *J. Phys. Chem.*, **87**, 3933 (1983).
6) L. R. Thorne, M. C. Branch, D. W. Chandler, R. J. Kee, and J. A. Miller, "21st Symp. Int. Combust., " The Combust. Inst., Pittsburg, PA, 1986, Abstr., p. 965.
7) D. A. Lichtin, M. R. Berman, and M. C. Lin, *Chem. Phys. Lett.*, **108**, 18 (1984).
8) H. F. Calcote, *Combust. Flame*, **42**, 215 (1981).
9) C. Vinkier, *J. Phys. Chem.*, **83**, 1234 (1979).
10) M. C. Lin, *J. Phys. Chem.*, **77**, 2726 (1973).
11) J. E. Butler, J. W. Fleming, L. P. Goss, and M. C. Lin, *Chem. Phys.*, **56**, 355 (1981).
12) M. R. Berman, J. W. Fleming, A. B. Harvey, and M. C. Lin, "19th Symp. Int. Combust., " The Combust. Inst., Pittsburg, PA, 1982, Abstr., p. 73.
13) S. S. Wagal, T. Carrington, S. V. Filseth, and C. M. Sadowski, *Chem. Phys.*, **69**, 61 (1982).
14) N. Nishiyama, H. Sekiya, S. Yamaguchi, M. Tsuji, and Y. Nishimura, *J. Phys. Chem.*, **90**, 1491 (1986).
15) A. J. Dean, R. K. Hanson, and C. T. Bowman, *J. Phys. Chem.*, **95**, 3180 (1991).
16) J. A. Miller and C. T. Bowman, *Prog. Energy Combust. Sci.*, **15**, 287 (1989).
17) A. M. Dean, *J. Phys. Chem.*, **89**, 4600 (1985).
18) J. W. Bozzelli, M. H. UI. Karim, and A. M. Dean, "Proc. 6th Toyota Conf. on Turbulence and Molecular Processes in Combustion, " Elsevier Publisher, (in press).
19) M. C. Lin, *J. Chem. Phys.*, **61**, 1835 (1974).
20) I. Messing, C. M. Sadowski, and S. V. Filseth, *Chem. Phys. Lett.*, **66**, 95 (1979).
21) J. A. Duncanson, Jr. and W. A. Guillory, *J. Chem. Phys.*, **78**, 4958 (1983).
22) S. M. Anderson, A. Freedman, and C. E. Kolb, *J. Phys. Chem.*, **91**, 6272 (1987).
23) K. H. Becker, B. Engelhardt, P. Wiesen, and K. D. Bayes, *Chem. Phys. Lett.*, **154**, 342 (1989).
24) W. A. Sanders and M. C. Lin, in "Chemical Kinetics of Small Organic Radicals, " ed by Z. B. Alfassi, CRC Press, Boca Raton, FL (1988), Chap. 14, and references therein.
25) R. König and J. Lademann, *Chem. Phys. Lett.*, **94**, 152 (1983).
26) B. M. Stone, M. Noble, and E. K. C. Lee, *Chem. Phys. Lett.*, **118**, 83 (1985); G. Rumbles, J. J. Valentini, B. M. Stone, and E. K. C. Lee, *J. Phys. Chem.*, **93**, 1303 (1989).
27) C. E. Moore and H. P. Broida, *J. Res. Natl. Bur. Stand., Sect. A*, **63A**, 19 (1959).
28) H. S. Liszt and W. H. Smith, *J. Quant. Spectrosc. Radiat. Transfer*, **12**, 947 (1972).
29) K. Yamasaki, S. Okada, M. Koshi, and H. Matsui, *J. Chem. Phys.*, **95**, 5087 (1991).
30) W. F. Cooper and J. F. Hershberger, *J. Phys. Chem.*, **96**, 771 (1992).
31) L. Hellner, K. T. V. Grattan, and M. H. R. Hutchinson, *Chem. Phys.*, **80**, 345 (1983).
32) K. P. Huber and G. Hertzberg, "Constants of Diatomic Molecules, " Van Nostrand Reinhold, New York (1979).
33) S. W. Benson, "Thermochemical Kinetics, " 2nd ed, John Wiley and Sons, New York (1976).
34) G. C. Schatz, M. S. Fitzcharles, and L. B. Harding, *Faraday Discuss. Chem. Soc.*, **84**, 359 (1987).